NACA TN 4307

NATIONAL ADVISORY COMMITTEE FOR AERONAUTICS

TECHNICAL NOTE 4307

EXPERIMENTAL MEASUREMENTS OF THE EFFECTS OF AIRPLANE MOTIONS ON WING AND TAIL ANGLES OF ATTACK OF A SWEPT-WING BOMBER IN ROUGH AIR

By Jerome N. Engel

Langley Aeronautical Laboratory
Langley Field, Va.

Washington
August 1958

NATIONAL ADVISORY COMMITTEE FOR AERONAUTICS

TECHNICAL NOTE 4307

EXPERIMENTAL MEASUREMENTS OF THE EFFECTS OF AIRPLANE MOTIONS ON WING AND TAIL ANGLES OF ATTACK OF A SWEPT-WING BOMBER IN ROUGH AIR

By Jerome N. Engel

SUMMARY

Flight test data obtained from a large swept-wing bomber airplane in flight through rough air at an altitude of 5,000 feet are analyzed to determine the effects of vertical translation and pitching motions on the angles of attack of the wing and tail. Power-spectral techniques are used to determine the contributions of these motions to the angles of attack of the wing and tail at various frequencies, and the results are compared with the direct gust-induced angle of attack.

The results indicate that the motions, particularly the pitching motions, significantly amplify the angles of attack of the wing and tail for the test airplane. The pitching-motion component increases the root-mean-square angle of attack of the wing by about 35 percent and the root-mean-square angle of attack of the tail by about 50 to 60 percent.

INTRODUCTION

The effects of airplane longitudinal motions, particularly the pitching motions, on the loads or angles of attack of the wing and tail of an airplane in flight through rough air have long been of concern. A number of analytic studies (for example, refs. 1 and 2) have indicated that the motions may contribute substantially to the airplane loading. The evaluation of these motion effects experimentally, however, has been complicated by the continuous and random character of both the turbulence and the resulting airplane motions. As a consequence, few experimental data exist on the subject.

As part of an investigation of the effects of airplane flexibility on the strains in rough air for a large swept-wing bomber airplane (ref. 3), time-history measurements of the vertical gust velocity and the longitudinal airplane motions were obtained. These measurements provided an opportunity for evaluating the effects of the longitudinal

motions on the loading or angles of attack of the wing and tail for the test airplane; consequently, an analysis of these measurements was undertaken. In the present report, power-spectral methods of analysis are applied to the test measurements in order to determine the direct contributions of the airplane vertical velocity and pitch responses to the angles of attack of the wing and tail at the various frequencies during flight in rough air. The techniques used in the analysis and the results obtained are presented.

SYMBOLS

A	truncated measure of the root mean square, $\left[\int_{.25}^{1.5} \Phi(f)df\right]^{1/2}$, radians
a_n	normal acceleration, g units
$d\epsilon/d\alpha$	downwash factor
f	frequency, cps
I	imaginary part of cross-spectrum
l_1	distance between angle-of-attack vane and center of gravity, ft
l_2	distance between center of gravity and root quarter-chord of horizontal tail, ft
l_3	distance between angle-of-attack vane and quarter-chord of horizontal tail, ft
M	Mach number
n	number of separate power estimates
R	real part of cross-spectrum
t_1	time for gust to travel from angle-of-attack vane to wing, sec
t_2	time for gust to travel from wing to horizontal tail, sec
t_3	time for gust to travel from angle-of-attack vane to horizontal tail, sec

V	airplane forward speed, ft/sec
w_a	airplane vertical velocity, ft/sec
w_g	vertical gust velocity, ft/sec
α_g	gust-induced angle of attack, radians
α_t	tail angle of attack as measured at quarter-chord of horizontal tail, radians
α_v	vane-indicated angle of attack, radians
α_w	wing angle of attack as measured at center of gravity, radians
γ	flight-path angle, $\frac{w_a}{V}$, radians
θ	pitch attitude, radians
$\dot{\theta}$	pitching velocity, radians/sec
Λ	wing sweep angle at quarter-chord line, deg
$\Phi_{ij}(f)$	power spectrum if $i = j$ or cross-spectrum if $i \neq j$, radians^2/cps (see ref. 4)
$\Phi_{\alpha_t}(f)$	power spectrum of tail angle of attack, radians^2/cps
$\Phi_{\alpha_w}(f)$	power spectrum of wing angle of attack, radians^2/cps

AIRPLANE, INSTRUMENTATION, AND TESTS

Airplane

The airplane used in this investigation was a six-engine jet bomber. The configuration of the standard airplane was changed slightly for the tests by the addition of an airspeed measuring boom and fairing on the nose and by an external canopy mounted on top of the fuselage to house an optigraph. A photograph of the airplane is shown in figure 1. A two-view drawing of the airplane, showing some of the pertinent dimensions, is shown in figure 2. Some of the airplane characteristics are presented in table I.

Instrumentation

The instruments pertinent to this study included an NACA air-damped recording accelerometer mounted near the center of gravity to measure normal acceleration. A standard NACA attitude-pitch recorder and a magnetically damped NACA turnmeter were installed near the center of gravity to record the pitch angle and pitching velocity, respectively. A mass-balanced metal flow-direction vane was mounted on the nose boom to obtain an indication of the instantaneous angle of attack of the airplane. An NACA 1/10-second chronometric timer was used to correlate all recordings. Table II presents a summary of the instrument characteristics and their associated accuracies.

Tests

The data for this study were obtained as part of an investigation of the effects of airplane flexibility on the wing strains of a large swept-wing airplane in rough air. These data consist of 4 minutes of time-history measurements of vertical gust velocity and longitudinal airplane motions, and the data were obtained in clear-air turbulence at an altitude of 5,000 feet at a Mach number of approximately 0.63. The test was made with "hands-off" control; that is, the pilot only corrected for large deviations of the airplane from the prescribed altitude and heading. An examination of the control position recorders indicated that the only movements of the elevator during the flight in rough air consisted of several small deflections applied gradually by the pilot in order to correct for deviation of the airplane from the prescribed altitude.

METHOD OF ANALYSIS

The basic method of analysis consists of first expressing the angles of attack of the wing and tail as a sum of the vertical gust velocity and the longitudinal motions (airplane vertical velocity and pitching motions). Then the contributions of the motions (vertical velocity and pitch) to the wing (or tail) angle of attack are obtained by comparing the total wing (or tail) angle of attack in rough air with the gust-induced angle of attack. Likewise, the effects of the individual components of the motions are obtained by comparing the direct gust-induced angle of attack with the angle of attack evaluated by neglecting first the pitching-motion component only and then the vertical velocity component only. The methods used to determine the effects of the motions on angles of attack of the wing and tail are described in the following sections.

Wing

Figure 3 shows the geometrical relations between the wing angle of attack, the airplane motions, and the vertical gust velocity. From the figure, it may be seen that the angle of attack of the wing (measured at the center line) in rough air is given by the following equations:

$$\alpha_w(t) = \theta(t) + \gamma(t) + \alpha_g(t)$$

$$= \theta(t) + \frac{w_a}{V}(t) + \frac{w_g}{V}(t) \qquad (1)$$

where

θ pitch attitude, radians

α_g gust-induced angle of attack, radians

γ flight-path angle, radians

w_a airplane vertical velocity, ft/sec

V airplane forward speed, ft/sec

w_g vertical gust velocity, ft/sec

t time

In the present investigation, measurements of the instantaneous vertical gust velocities were made by the use of an angle-of-attack vane mounted on a boom at a distance l_1 of 52.5 feet ahead of the airplane center of gravity. Thus, the wing penetrates the gust w_g at a time $t_1 = \frac{l_1}{V}$ after the vane penetrates the gust, and this time lag must be taken into account in order to use the measured gust velocities in equation (1). By introducing this time lag factor into equation (1), the instantaneous angle of attack of the wing may be expressed as

$$\alpha_w(t) = \theta(t) + \frac{w_a}{V}(t) + \frac{w_g}{V}(t-t_1) \qquad (2)$$

Tail

The angle of attack at the tail may be obtained from the angle of attack of the wing by taking into account the effects of pitching velocity, wing downwash, and the appropriate time lags. In rough air, the instantaneous angle of attack of the tail $\alpha_t(t)$ may be expressed as

$$\alpha_t(t) = \alpha_w(t) - \alpha_w(t-t_2)\frac{d\epsilon}{d\alpha} + \alpha_g(t-t_3) - \alpha_g(t-t_1) + \frac{l_2}{V}\dot{\theta}(t)$$

$$= \theta(t) + \frac{w_a}{V}(t) - \theta(t-t_2)\frac{d\epsilon}{d\alpha} - \frac{w_a}{V}(t-t_2)\frac{d\epsilon}{d\alpha} + \frac{w_g}{V}(t-t_3) -$$

$$\frac{w_g}{V}(t-t_3)\frac{d\epsilon}{d\alpha} + \frac{l_2}{V}\dot{\theta}(t) \qquad (3)$$

where

$\frac{d\epsilon}{d\alpha}$ downwash factor

t_2 time gust takes in traveling from airplane center of gravity to quarter-chord of horizontal tail, l_2/V

t_3 time gust takes to travel from vane to quarter-chord of horizontal tail, l_3/V

The downwash factor $d\epsilon/d\alpha$ used in equation (3) was estimated from the following empirical relation derived from flight test data for this airplane in reference 5:

$$\left(\frac{d\epsilon}{d\alpha}\right)_{M\leq.70} = \frac{0.458}{\sqrt{1 - M^2\cos^2\Lambda}}$$

For the present investigation where $M = 0.63$ and $\Lambda = 35^\circ$,

$$\frac{d\epsilon}{d\alpha} \approx 0.5$$

Power-Spectra Equations

In order to examine the contributions of the motions to the wing- and tail-angle-of-attack responses at the various frequencies, power spectra of the angle-of-attack variations for various conditions are determined. The power spectra of the wing and tail angles of attack may be obtained from equations (2) and (3) by either of two procedures. First, the equations may be evaluated to obtain time histories of the wing and tail angles of attack from which the power spectra may be calculated. Secondly, equations (2) and (3) may be transformed so as to express the power spectra of the wing and tail angles of attack in terms of the power-spectra and cross-spectra components of the motions and gust velocity. The second procedure is used herein.

The power spectra of the angle of attack of the wing $\Phi_{\alpha_w}(f)$ and of the tail $\Phi_{\alpha_t}(f)$ may, from equations (2) and (3), respectively, be expressed as

$$\Phi_{\alpha_w}(f) = \left[\Phi_\theta(f)\right] + \frac{1}{V^2}\left[\Phi_{w_a}(f)\right] + \frac{1}{V^2}\left[\Phi_{w_g}(f)\right] + \frac{2}{V} R\left[\Phi_{w_a\theta}(f)\right] +$$

$$\frac{2}{V} R\left[\Phi_{w_g\theta}(f)\right] \cos 2\pi f t_1 - \frac{2}{V} I\left[\Phi_{w_g\theta}(f)\right] \sin 2\pi f t_1 +$$

$$\frac{2}{V^2} R\left[\Phi_{w_a w_g}(f)\right] \cos 2\pi f t_1 - \frac{2}{V^2} I\left[\Phi_{w_a w_g}(f)\right] \sin 2\pi f t_1 \qquad (4)$$

and

$$\Phi_{\alpha_t}(f) = \left[\Phi_\theta(f)\right]\left(1.25 - \cos 2\pi f t_2\right) + \frac{1}{V^2}\left[\Phi_{w_a}(f)\right]\left(1.25 - \cos 2\pi f t_2\right) +$$

$$\frac{0.25}{V^2}\left[\Phi_{w_g}(f)\right] + \frac{l_2^2}{V^2}\left[\Phi_{\dot\theta}(f)\right] + \frac{2}{V} R\left[\Phi_{w_a\theta}(f)\right]\left(1.25 - \cos 2\pi f t_2\right) +$$

$$\frac{2}{V} R\left[\Phi_{w_g\theta}(f)\right]\left[0.5 \cos 2\pi f t_3 - 0.25 \cos 2\pi f(t_3 - t_2)\right] +$$

$$\frac{2}{V} I\left[\Phi_{w_g\theta}(f)\right]\left[-0.5 \sin 2\pi f t_3 + 0.25 \sin 2\pi f(t_3 - t_2)\right] +$$

$$\frac{2}{V^2} R\left[\Phi_{w_a w_g}(f)\right]\left[0.5 \cos 2\pi f t_3 - 0.25 \cos 2\pi f(t_3 - t_2)\right] +$$

$$\frac{2}{V^2} I\left[\Phi_{w_a w_g}(f)\right]\left[0.5 \sin 2\pi f t_3 - 0.25 \sin 2\pi f(t_3 - t_2)\right] +$$

$$\frac{2l_2}{V^2} R\left[\Phi_{w_a\dot\theta}(f)\right]\left(1 - 0.5 \cos 2\pi f t_2\right) + \frac{l_2}{V^2} I\left[\Phi_{w_a\dot\theta}(f)\right]\left(\sin 2\pi f t_2\right) +$$

$$\frac{l_2}{V^2} R\left[\Phi_{w_g\dot\theta}(f)\right]\left(\cos 2\pi f t_3\right) - \frac{l_2}{V^2} I\left[\Phi_{w_g\dot\theta}(f)\right]\left(\sin 2\pi f t_3\right) \qquad (5)$$

where

R real part of cross-spectrum

I imaginary part of cross-spectrum

Equations (4) and (5) express the contributions of the spectra and cross-spectra of the various motions and gust velocity to the power spectra of the wing and tail angles of attack, respectively. The direct contributions of the airplane motions to the wing and tail angles of attack may be ascertained by comparing $\Phi_{\alpha_w}(f)$ and $\Phi_{\alpha_t}(f)$ obtained from equations (4) and (5), respectively, with the power spectra of the

gust-induced angle of attack. The direct contributions of the gust to the power spectra of the wing and tail angles of attack are given by the terms $\frac{1}{V^2}\left[\Phi_{w_g}(f)\right]$ and $\frac{0.25}{V^2}\left[\Phi_{w_g}(f)\right]$ in equations (4) and (5), respectively. The spectral effects of vertical velocity and pitch on the wing and tail angles of attack may be determined by omitting the terms involving either θ or w_a in equations (4) and (5) and then by comparing the resulting spectra with the direct gust-induced angle-of-attack spectra.

EVALUATION OF DATA AND RESULTS

The record evaluation consisted of reading the measured time histories of pitching velocity $\dot{\theta}$, vane-indicated angle of attack α_v, and the center-of-gravity normal acceleration a_n at given time intervals. The reading interval was 0.1 second for $\dot{\theta}$ and α_v and 0.05 second for a_n. The values of $\dot{\theta}$ and a_n were numerically integrated in order to obtain time histories of the pitch angle θ and the airplane vertical velocity w_a. The values of $\dot{\theta}$, θ, w_a, and α_v were used to determine the time history of the vertical gust velocity w_g in accordance with the general method given in reference 6. The detailed procedures used in the gust-velocity determination are presented in reference 7.

The time-history values of θ, $\dot{\theta}$, w_a, and w_g were used to calculate the various power spectra and cross-spectra required in the right-hand side of equations (4) and (5). These calculations were based on the methods given in reference 8. In calculating the various power spectra and cross-spectra, 60 lagged products ($n = 60$) and $\Delta t = 0.1$ second were used so that 60 power estimates were obtained between 0 and 5 cps. Only the results for the frequency range of 0.25 cps to 1.5 cps are used herein, however, for the following reasons:

(1) This frequency range is of primary concern since most of the airplane loading is concentrated within the frequency range of 0.25 to 1.5 cps. This may be seen from examination of the power spectrum of normal acceleration at the center of gravity given in figure 4, which, as indicated in reference 3, provides a measure of the airplane loading.

(2) At frequencies below 0.25 cps, the power spectrum of vertical gust velocity obtained from the vane measurements is not considered reliable.

(3) At frequencies above 1.5 cps, the airplane pitching and vertical-velocity motions are small.

Tables III and IV present the individual power estimates of the power spectra and cross-spectra of the motions and gust velocity which contribute to the power spectra of the wing and tail angles of attack, as indicated by equations (4) and (5), respectively.

Three estimates for $\Phi_{\alpha_w}(f)$ and $\Phi_{\alpha_t}(f)$ are given in tables III and IV, respectively. These spectra were obtained by: (1) summing all the terms in tables III and IV according to equations (4) and (5), (2) neglecting the terms involving only θ and $\dot{\theta}$, and (3) neglecting the terms involving only w_a. The three spectra of α_w and α_t are also given in figures 5 and 6, respectively. In addition, the power spectra of the direct gust-induced angle of attack of the wing and tail are given in these figures. The contributions of the gust to the power spectrum of the angle of attack of the wing is given by the term $\frac{1}{V^2}\left[\Phi_{w_g}(f)\right]$ in table III. For the tail, the spectrum of the gust-induced angle of attack is given by the term $\frac{0.25}{V^2}\left[\Phi_{w_g}(f)\right]$ in table IV.

Comparison of the various spectra in figures 5 and 6 provides an indication of the contributions at the various frequencies of the direct gust effects, vertical motions, and the pitching motions to the angle-of-attack spectra of the wing and tail. As an indication of the total power, the values of the quantity A, defined by

$$A = \left[\int_{.25}^{1.5} \Phi(f)df\right]^{1/2}$$

is also given in figures 5 and 6. The values of A may be considered a truncated estimate of the root-mean-square angle of attack because only the power over the frequency range of 0.25 cps to 1.5 cps was considered.

RELIABILITY OF RESULTS

The present results are subject to errors due to a number of factors. The more important ones appear to be:

(a) The accuracy of the basic measurements

(b) The accuracy of the gust-velocity determination

(c) Possible errors arising from airplane flexibility, particularly in regard to fuselage bending affecting the tail angle of attack

(d) Inaccuracies in the determination of the downwash factor $d\epsilon/d\alpha$

(e) Statistical sampling errors

The reliability of the present measurements and the gust-velocity determination was considered in detail in another connection in reference 7. The results obtained therein suggest that the measurements and the gust velocity are sufficiently accurate for present purposes for the frequency range considered. The possible effects of fuselage flexibility on the tail angle of attack were also considered. An evaluation of these effects, based on the results of reference 9, indicates that these effects are negligible for present purposes over most of the frequency region of concern. In order to determine the effects of inaccuracies in the downwash factor, the spectrum of the tail angle of attack was computed by using a 20-percent-lower downwash factor. The results obtained indicate that the 20-percent reduction in the downwash factor yielded a 15-percent increase in the spectrum of the tail angle of attack.

In order to establish the statistical reliability of the present results, the methods of reference 10 were used to obtain confidence bands for the present power-spectra and root-mean-square values. The results obtained indicated that each of the present power estimates is reliable to within about ±30 percent of the values given whereas the root-mean-square values are reliable to better than ±10 percent. In addition to the absolute reliability of the present power spectra, the reliability of ratios of the power estimates for the various power spectra is also of concern in the interpretation of the present results. Unfortunately, no means are yet available for establishing quantitative estimates of the reliability of ratios of power estimates, although the theoretical analysis and some of the results obtained in reference 11 indicate that such ratios may have greater statistical stability than the stability of individual spectral estimates.

DISCUSSION

Wing

Comparison of the power spectrum of the direct gust-induced angle of attack $\Phi_{\alpha_g}(f)$ with the power spectrum of the actual angle-of-attack

change of the wing $\Phi_{\alpha_w}(f)$ in figure 5 indicates that the combined airplane motions (pitch and vertical velocity) contribute significantly to the wing angle of attack over the frequency range 0.35 cps to 1.5 cps. Except for the small reduction in the wing angle-of-attack spectrum at frequencies below 0.35 cps, the motions tend to increase the spectrum of the gust-induced angle-of-attack change at the wing by factors of 2 and 3 over the entire frequency range. The overall effects of the airplane motions, as indicated by the values of A, cause about a 30-percent amplification of the gust-induced angle of attack over the frequency range of 0.25 to 1.5 cps.

Comparison in figure 5 of the spectrum of the wing angle of attack obtained by considering only the airplane vertical velocity ($\theta = 0$) with the gust-induced angle-of-attack spectrum $\Phi_{\alpha_g}(f)$ shows that the vertical velocity component acts to reduce the net angle of attack at frequencies below 0.6 cps. Above this frequency, however, the vertical velocity component of the angle of attack adds to the gust-induced angle of attack. The overall effect of the vertical velocity component is a small reduction in the wing angle-of-attack change, as is indicated by the values of A. The pitching-motion component, however, adds to the gust-induced angle of attack over almost the entire frequency range and gives an overall increase in airplane angle of attack of about 35 percent.

Tail

Examination of figure 6 indicates that the overall effects of the airplane motions on the tail angle of attack are of the same general character as for the wing angle of attack and act to increase the angle of attack over the entire frequency range. The magnitude of the increase is, however, greater for the angle of attack of the tail and increases the direct gust-induced angle-of-attack variations by about 70 percent. Further examination of figure 6 indicates that the effect of the airplane vertical-motion component on the tail angle of attack opposes the gust-induced angle of attack at the lower frequencies (below 0.50 cps) but adds to the angle of attack at the higher frequencies. The overall effects of the vertical-motion component on the tail angle of attack appear to be small, as is indicated by a comparison of the values of A given in figure 6. The pitching-motion component (both pitch attitude and pitching velocity), however, significantly increases the power spectrum of the tail angle of attack for the entire frequency range covered. This increase amounts to 50 to 60 percent for the overall angle-of-attack variations, as is shown by the values of A.

CONCLUDING REMARKS

The foregoing analysis of the longitudinal airplane motions (pitch and vertical velocity) of a large swept-wing bomber airplane in rough air have served to indicate that the motions in rough air have an appreciable effect on both wing and tail angles of attack. For the test airplane, the effects of the airplane vertical velocity appear to be relatively small. The effects of the pitching motions, however, are unfavorable and tend to increase the direct gust-induced angle of attack over almost the entire frequency range (0.25 to 1.5 cps). The overall effect of the pitching motion appears to increase the root-mean-square wing angle of attack by about 35 percent over the direct gust effects. The overall effect of the pitching motion on the tail angle of attack appears to be even larger and increases the root-mean-square angle of attack by about 50 to 60 percent.

Langley Aeronautical Laboratory,
National Advisory Committee for Aeronautics,
Langley Field, Va., May 8, 1958.

REFERENCES

1. Donely, Philip: Summary of Information Relating to Gust Loads on Airplanes. NACA Rep. 997, 1950. (Supersedes NACA TN 1976.)

2. Pratt, Kermit G., and Bennett, Floyd V.: Charts for Estimating the Effects of Short-Period Stability Characteristics on Airplane Vertical-Acceleration and Pitch-Angle Response in Continuous Atmospheric Turbulence. NACA TN 3992, 1957.

3. Rhyne, Richard H., and Murrow, Harold N.: Effects of Airplane Flexibility on Wing Strains in Rough Air at 5,000 Feet As Determined by Flight Tests of a Large Swept-Wing Airplane. NACA TN 4107, 1957.

4. Press, Harry: Atmospheric Turbulence Environment With Special Reference to Continuous Turbulence. Presented to Structures and Materials Panel of AGARD (Copenhagen, Denmark), Apr. 29 - May 4, 1957.

5. Aiken, William S., Jr., and Fisher, Raymond A.: Horizontal-Tail Parameters As Determined From Flight-Test Tail Loads on a Flexible Swept-Wing Jet Bomber. NACA RM L56J02, 1957.

6. Chilton, Robert G.: Some Measurements of Atmospheric Turbulence Obtained From Flow-Direction Vanes Mounted on an Airplane. NACA TN 3313, 1954.

7. Coleman, Thomas L., Press, Harry, and Meadows, May T.: An Evaluation of Effects of Flexibility on Wing Strains in Rough Air for a Large Swept-Wing Airplane by Means of Experimentally Determined Frequency-Response Functions With an Assessment of Random-Process Techniques Employed. NACA TN 4291, 1958.

8. Press, Harry, and Tukey, John W.: Power Spectral Methods of Analysis and Their Application to Problems in Airplane Dynamics. Vol. IV of AGARD Flight Test Manual, Pt. IV C, Enoch J. Durbin, ed., North Atlantic Treaty Organization, pp. IVC:1 - IVC:41.

9. Mayo, Alton P.: Flight Investigation and Theoretical Calculations of the Fuselage Deformations of a Swept-Wing Bomber During Push-Pull Maneuvers. NACA RM L56L05, 1957.

10. Press, Harry, and Houbolt, John C.: Some Applications of Generalized Harmonic Analysis to Gust Loads on Airplanes. Jour. Aero. Sci., vol. 22, no. 1, Jan. 1955, pp. 17-26, 60.

11. Goodman, N. R.: On the Joint Estimation of the Spectra, Cospectrum and Quadrature Spectrum of a Two-Dimensional Stationary Gaussian Process. Scientific Paper No. 10 (BuShips Contract Nobs-72018 (1734-F) and David Taylor Model Basin Contract Nonr-285 (17)), Eng. Statistics Lab., New York Univ., Mar. 1957.

TABLE I

PERTINENT PHYSICAL CHARACTERISTICS AND DIMENSIONS

OF THE TEST AIRPLANE

Wing:	
Total area, sq ft	1,428
Span, ft	116
Aspect ratio	9.43
Thickness ratio	0.12
Taper ratio	0.42
Mean aerodynamic chord, in.	155.9
Sweepback at 25-percent-chord line, deg	35
Horizontal Tail:	
Total area, sq ft	268
Span, ft	33
Mean aerodynamic chord, in.	102.9
Sweepback at 25-percent-chord line, deg	35
Airplane weight, lb	113,000

TABLE II

SUMMARY OF INSTRUMENT CHARACTERISTICS AND ACCURACIES

Quantity measured	Measurement station	Instrument range	Instrument sensitivity	Estimated instrument accuracy
Normal acceleration, g units	34.2 percent mean aerodynamic chord	±1.0	1.01 $\frac{\text{g units}}{\text{in.}}$	0.005
Pitching velocity, radians/sec	25.0 percent mean aerodynamic chord	±0.25	0.254 $\frac{\text{radians/sec}}{\text{in.}}$	0.005
Vane-indicated angle of attack, radians	79 in. ahead of original nose	±0.5	0.183 $\frac{\text{radians}}{\text{in.}}$	0.002
Time, sec	----------	-----	----------	0.005

TABLE III.- CONTRIBUTIONS OF THE VARIOUS TERMS OF EQUATION (4) TO THE POWER SPECTRUM OF THE WING ANGLE OF ATTACK, AS A FUNCTION OF FREQUENCY

Terms of equation (4)	Contribution of various terms, $(\text{radians})^2/\text{cps}$, at frequency of -															
	0.25 cps	0.333 cps	0.417 cps	0.50 cps	0.583 cps	0.667 cps	0.75 cps	0.833 cps	0.917 cps	1.0 cps	1.083 cps	1.167 cps	1.25 cps	1.333 cps	1.417 cps	1.50 cps
$\Phi_\theta(f)$	223.0×10^{-7}	123.0×10^{-7}	76.7×10^{-7}	69.0×10^{-7}	52.5×10^{-7}	30.3×10^{-7}	19.7×10^{-7}	14.1×10^{-7}	10.9×10^{-7}	7.20×10^{-7}	3.34×10^{-7}	3.38×10^{-7}	4.38×10^{-7}	3.89×10^{-7}	2.99×10^{-7}	3.22×10^{-7}
$\frac{1}{V^2}\left[\Phi_{w_a}(f)\right]$	69.9	54.1	35.5	35.0	24.2	12.7	7.57	4.76	3.34	2.48	1.32	.887	.845	.814	.645	.598
$\frac{1}{V^2}\left[\Phi_{w_g}(f)\right]$	342.0	166.0	110.0	94.0	59.8	37.5	32.5	24.5	19.0	17.5	16.6	15.7	17.1	16.5	12.8	12.4
$\frac{2}{V} R\left[\Phi_{w_a\theta}(f)\right]$	159.0	66.8	39.6	22.0	12.1	.999	-.743	-3.05	-4.56	-4.05	-2.20	-1.74	-2.56	-3.05	-2.46	-1.91
$\frac{2}{V} R\left[\Phi_{w_g\theta}(f)\right]\cos 2\pi f t_1$	-338.0	-119.0	-22.3	29.2	42.2	40.1	33.9	25.0	17.8	14.2	11.2	9.06	8.97	8.42	5.11	3.26
$-\frac{2}{V} I\left[\Phi_{w_g\theta}(f)\right]\sin 2\pi f t_1$	35.2	31.6	31.0	32.3	22.2	10.7	5.70	2.44	.00203	-2.16	-2.79	-3.64	-5.78	-6.23	-3.42	-5.49
$\frac{2}{V^2} R\left[\Phi_{w_a w_g}(f)\right]\cos 2\pi f t_1$	-264.0	-147.0	-105.0	-88.6	-51.6	-23.2	-13.0	-7.22	-3.19	-.450	-.0102	.631	2.20	2.38	1.75	1.53
$-\frac{2}{V^2} I\left[\Phi_{w_a w_g}(f)\right]\sin 2\pi f t_1$	2.10	2.69	5.70	10.2	10.7	9.83	4.50	7.37	5.78	5.25	5.27	4.58	5.13	5.07	3.50	2.69
$\Phi_{\alpha_w}(f)$	229.0	177.0	172.0	203.0	172.0	118.0	90.1	67.9	49.1	39.9	32.7	28.9	30.3	27.8	20.9	16.3
$\Phi_{\alpha_w}(f)$ $(\theta = 0)$	149.0	74.9	46.8	50.6	43.1	36.9	31.6	29.4	24.9	24.8	23.2	21.8	25.3	24.7	18.7	17.2
$\Phi_{\alpha_w}(f)$ $(w_a = 0)$	260.0	201.0	196.0	225.0	177.0	119.0	91.8	66.1	47.7	36.7	28.3	24.5	24.7	22.6	17.4	13.3

TABLE IV.- CONTRIBUTIONS OF THE VARIOUS TERMS OF EQUATION (5) TO THE POWER SPECTRUM OF THE TAIL ANGLE OF ATTACK, AS A FUNCTION OF FREQUENCY

Terms of equation (5)	Contribution of various terms, $(\text{radians})^2/\text{cps}$, at frequency of -														
	0.25 cps	0.333 cps	0.417 cps	0.50 cps	0.583 cps	0.667 cps	0.75 cps	0.833 cps	0.917 cps	1.0 cps	1.083 cps	1.167 cps	1.25 cps	1.333 cps	1.417 cps	1.50 cps
$\Phi_\theta(f)\left(1.25 - \cos 2\pi f t_2\right)$	57.0×10^{-7}	31.9×10^{-7}	20.3×10^{-7}	18.7×10^{-7}	14.7×10^{-7}	8.73×10^{-7}	5.88×10^{-7}	4.38×10^{-7}	3.52×10^{-7}	2.42×10^{-7}	1.17×10^{-7}	1.24×10^{-7}	1.67×10^{-7}	1.55×10^{-7}	1.25×10^{-7}	1.41×10^{-7}
$\frac{1}{V^2}\left[\Phi_{w_a}(f)\right]\left(1.25 - \cos 2\pi f t_2\right)$	17.9	14.0	9.40	9.50	6.78	3.64	2.26	1.47	1.07	.831	.464	.324	.324	.326	.271	.263
$\frac{0.25}{V^2}\left[\Phi_{w_g}(f)\right]$	85.5	41.4	27.6	23.5	14.9	9.38	8.12	6.15	4.74	4.38	4.15	3.93	4.27	4.11	3.19	3.09
$\frac{l_2^2}{V^2}\left[\Phi_{\dot\theta}(f)\right]$	2.22	2.32	2.58	3.28	3.03	2.30	1.82	1.30	1.10	.920	.663	.698	1.03	1.15	.946	.853
$\frac{2}{V}R\left[\Phi_{w_a\theta}(f)\right]\left(1.25 - \cos 2\pi f t_2\right)$	40.6	17.3	10.5	5.98	3.39	.289	-.222	-.944	-1.47	-1.36	-.769	-.637	-.983	-1.22	-1.03	-.838
$\frac{2}{V}R\left[\Phi_{w_g\theta}(f)\right]\left[.5\cos 2\pi f t_3 - .25\cos 2\pi f(t_3 - t_2)\right]$	-81.4	-27.9	-5.03	6.27	8.51	7.47	5.74	3.74	2.28	1.48	.897	.446	.159	-.139	-.275	-.305
$\frac{2}{V}I\left[\Phi_{w_g\theta}(f)\right]\left[-.5\sin 2\pi f t_3 + .25\sin 2\pi f(t_3 - t_2)\right]$	24.0	21.6	20.8	21.7	14.7	7.02	3.66	1.54	.00142	-1.30	-1.64	-2.08	-3.22	-3.34	-1.78	-2.75
$\frac{2}{V^2}R\left[\Phi_{w_aw_g}(f)\right]\left[.5\cos 2\pi f t_3 - .25\cos 2\pi f(t_3 - t_2)\right]$	-63.8	-34.6	-23.6	-19.0	-10.4	-4.31	-2.20	-1.08	-.407	-.0468	-.000814	.0311	.0389	-.0395	-.0936	-.144
$\frac{2}{V^2}I\left[\Phi_{w_aw_g}(f)\right]\left[.5\sin 2\pi f t_3 - .25\sin 2\pi f(t_3 - t_2)\right]$	1.43	1.83	3.87	6.84	7.08	6.41	5.86	4.64	3.58	3.17	2.93	2.63	2.85	2.73	1.82	1.34
$\frac{2l_2}{V^2}R\left[\Phi_{w_a\dot\theta}(f)\right]\left(1 - .5\cos 2\pi f t_2\right)$	8.04	9.12	7.79	9.87	8.57	5.80	4.01	2.93	2.10	1.67	.922	.853	1.01	1.19	.788	.637
$\frac{l_2}{V^2}I\left[\Phi_{w_a\dot\theta}(f)\right]\left(\sin 2\pi f t_2\right)$	-.859	-.643	-.594	-.472	-.352	-.0383	.0358	.180	.326	.342	.216	.198	.334	.448	.403	.350
$\frac{l_2}{V^2}R\left[\Phi_{w_g\dot\theta}(f)\right]\left(\cos 2\pi f t_3\right)$	15.2	13.5	12.8	13.0	8.65	4.01	2.03	.822	.000610	-.623	-.737	-.865	-1.21	-1.11	-.798	-.629
$-\frac{l_2}{V^2}I\left[\Phi_{w_g\dot\theta}(f)\right]\left(\sin 2\pi f t_3\right)$	-3.91	-2.44	-.714	1.35	2.63	3.28	3.48	3.17	2.73	2.56	2.44	2.22	2.52	2.69	1.83	1.30
$\Phi_{a_t}(f)$	102.0	87.6	85.7	101.0	82.1	54.0	40.5	28.3	19.6	14.4	10.7	8.98	8.79	8.34	6.52	4.58
$\Phi_{a_t}(f)$ $(\theta = 0;\ \dot\theta = 0)$	40.9	22.7	17.3	20.9	18.4	15.1	14.0	11.2	8.99	8.34	7.55	6.90	7.49	7.12	5.19	4.56
$\Phi_{a_t}(f)$ $(w_a = 0)$	98.5	80.4	78.4	87.9	67.1	42.2	30.7	21.1	14.4	9.85	6.94	5.58	5.23	4.90	4.38	2.97

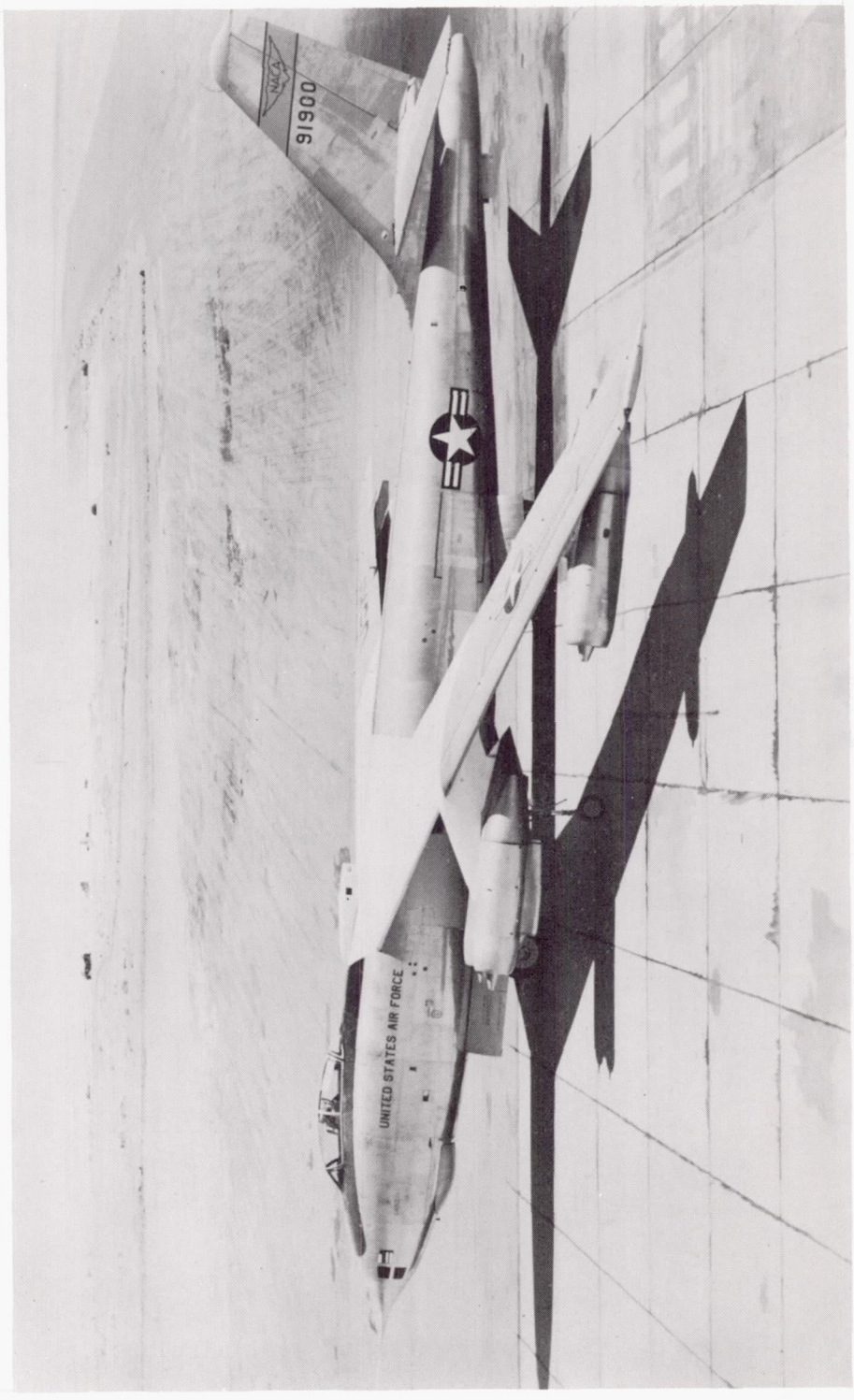

Figure 1.- Photograph of test airplane. L-86692

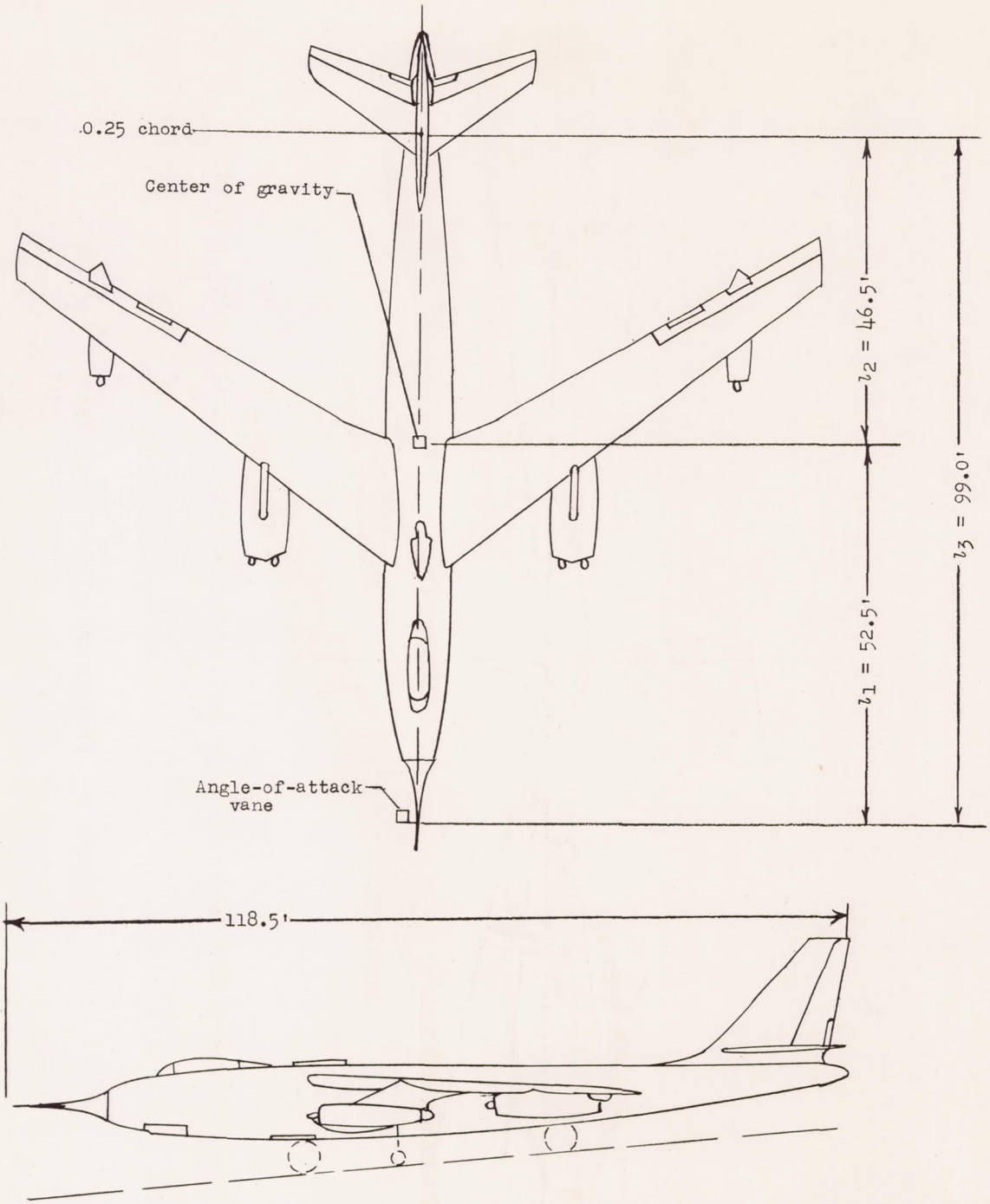

Figure 2.- Two-view drawing of test airplane.

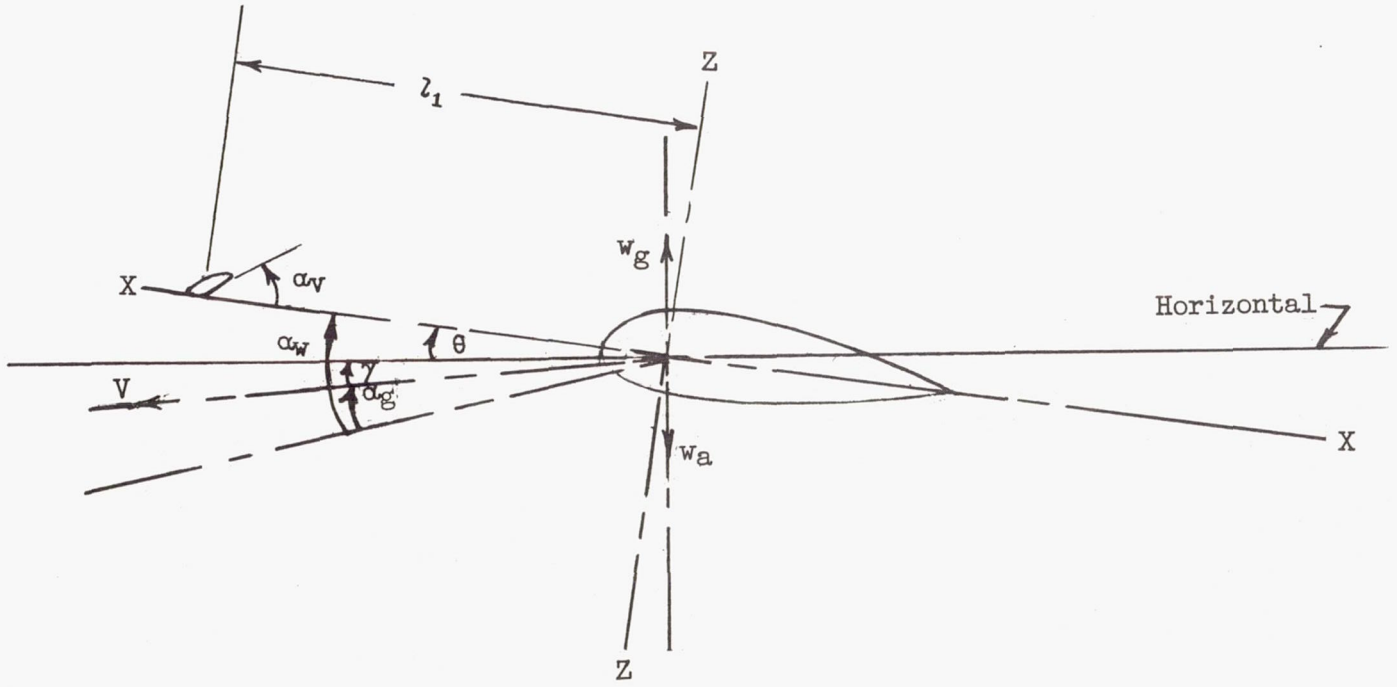

Figure 3.- Geometrical relations of the airplane motions with positive directions shown.

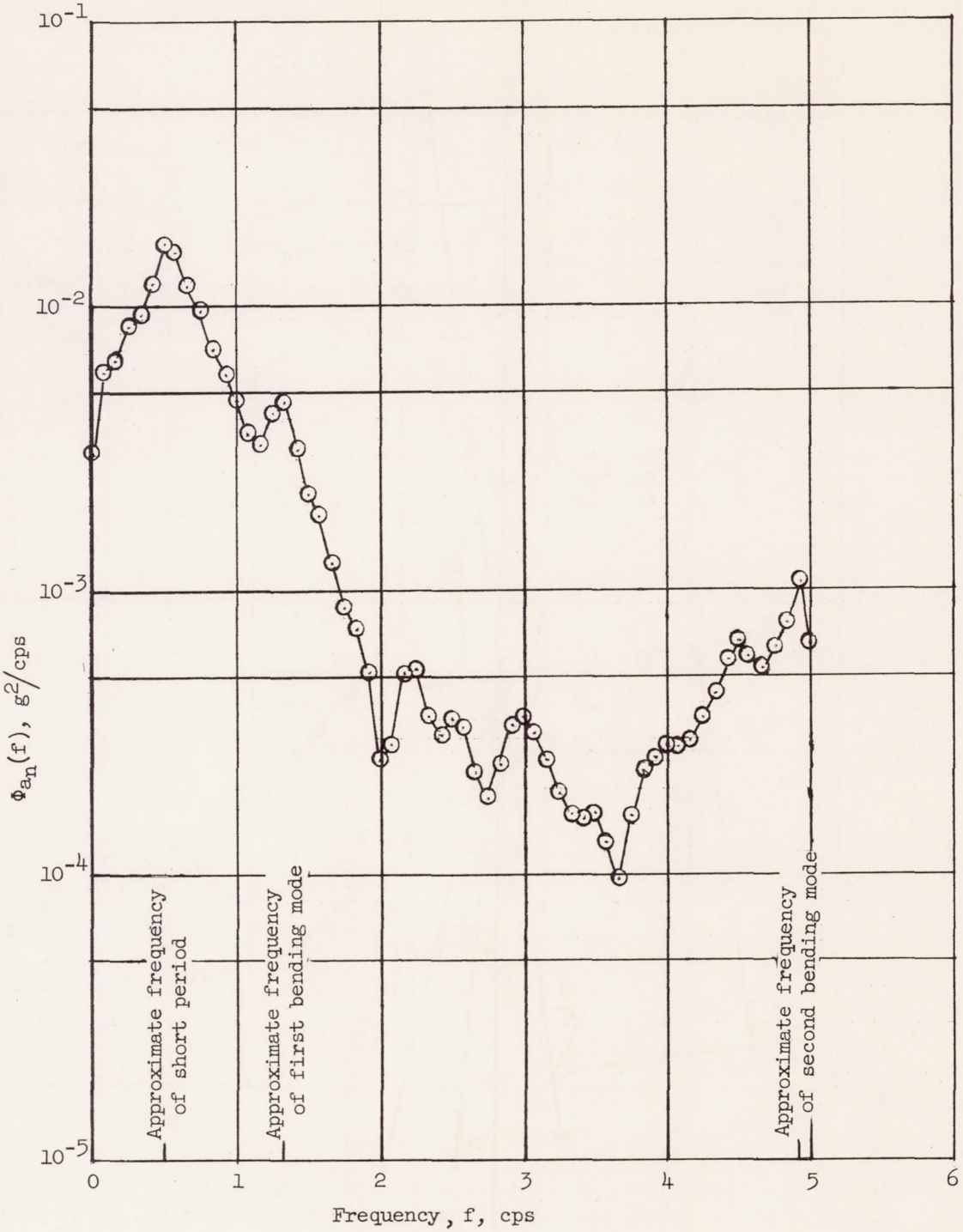

Figure 4.- Power spectrum of normal acceleration at the center of gravity.

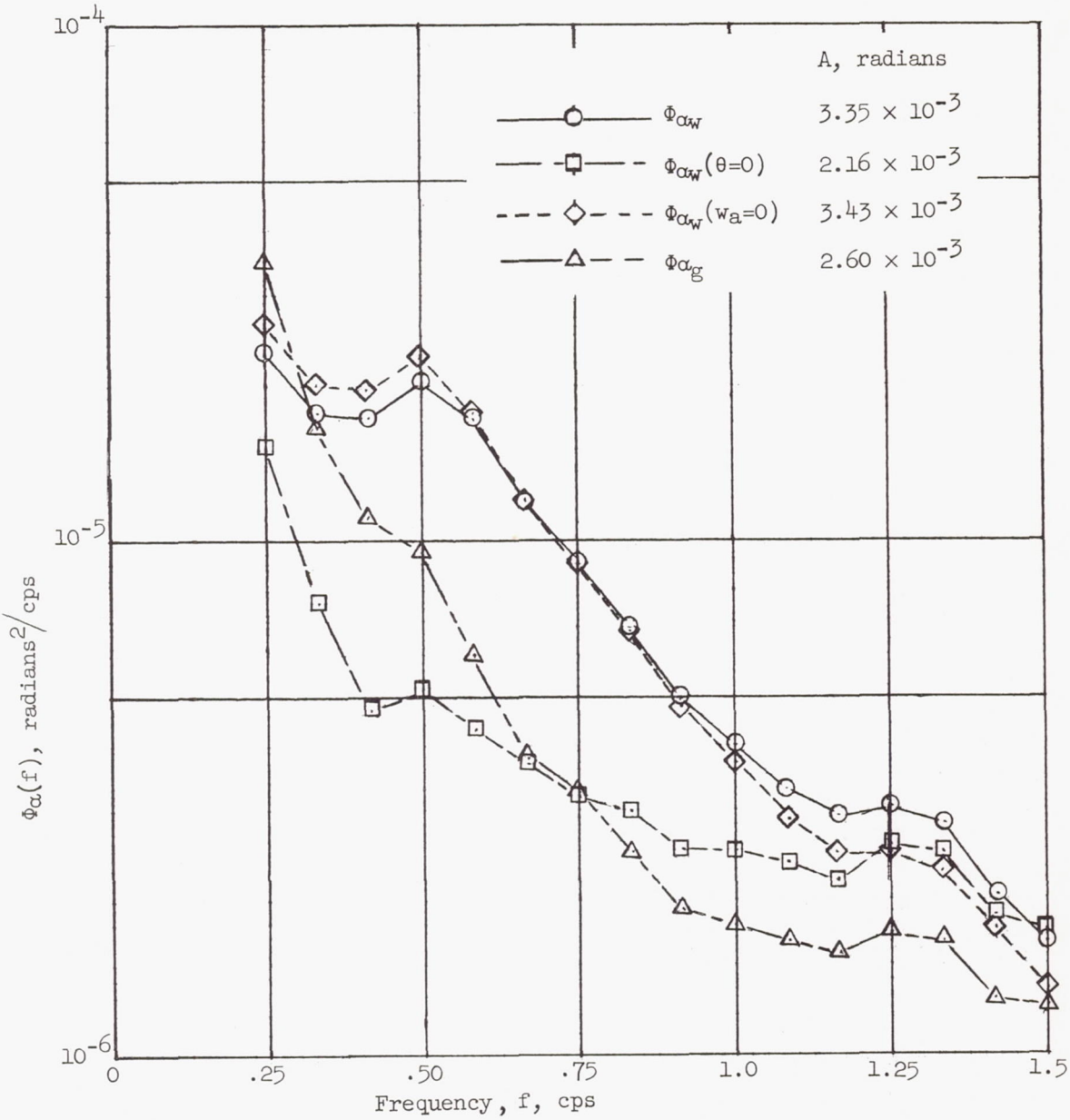

Figure 5.- Comparison of power spectra of wing angle of attack, with and without vertical- and pitching-motion components, with power spectrum of gust-induced angle of attack.

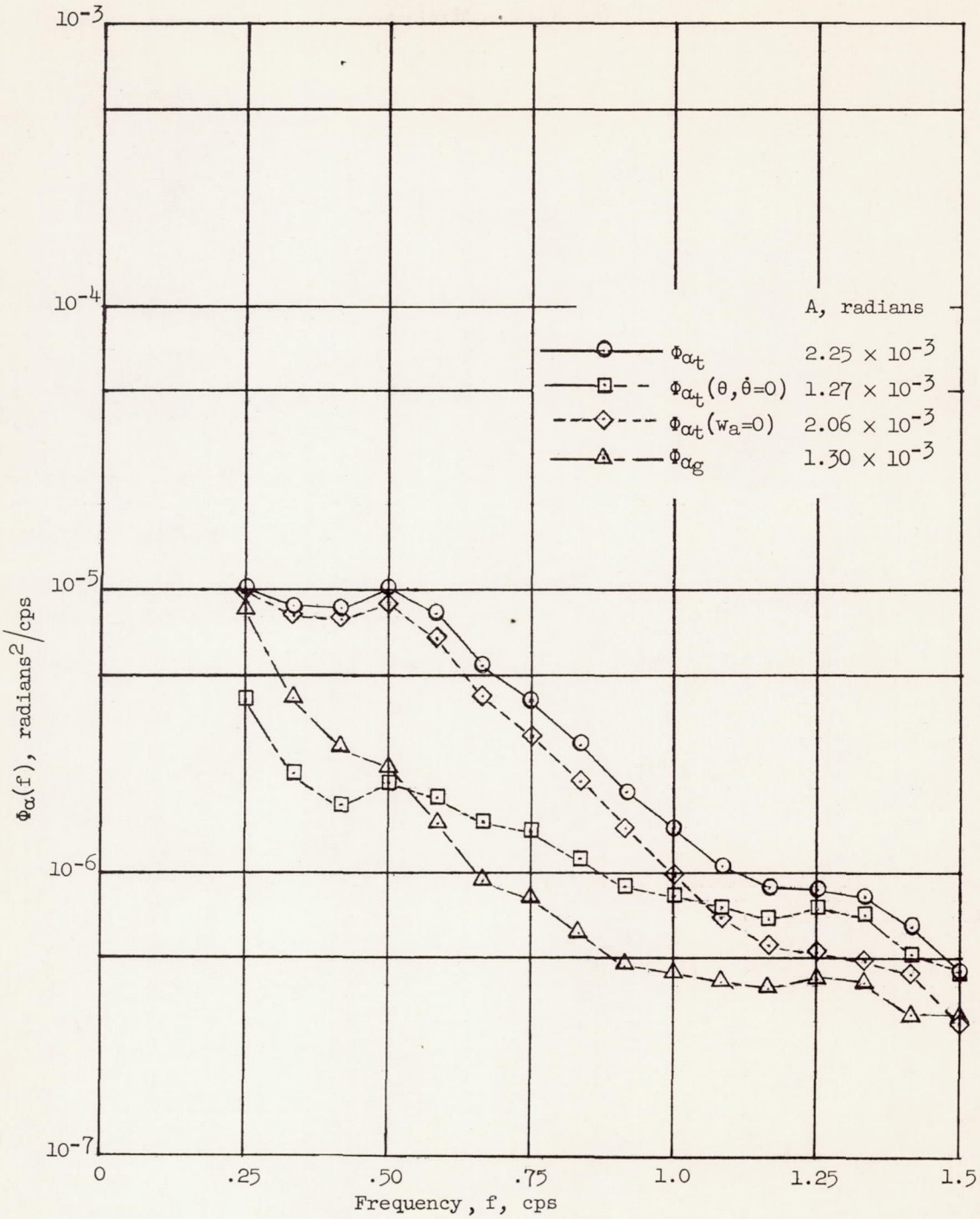

Figure 6.- Comparison of power spectra of tail angle of attack, with and without vertical- and pitching-motion components, with power spectrum of gust-induced angle of attack.